Image registration based on evidential reasoning

Deqiang Han
Center for Information Engineering Science Research
Xi'an Jiaotong University
Xi'an, China 710049
deqhan@gmail.com

Jean Dezert
ONERA
The French Aerospace Lab
Chemin de la Hunière
F-91761 Palaiseau, France
jean.dezert@onera.fr

Shicheng Li, Chongzhao Han
Inst. of Integrated Automation
MOE KLINNS Lab
Xi'an Jiaotong University
Xi'an, China 710049
czhan@mail.xjtu.edu.cn

Yi Yang
SKLSVMS
School of Aerospace
Xian Jiaotong University
Xian, China 710049
jiafeiyy@mail.xjtu.edu.cn

***Abstract*—Image registration is a crucial and necessary step before image fusion. It aims to achieve the optimal match between two or more images of the same scene taken at different times, from different viewpoints, and/or by different sensors. In the procedure of image registration, several types of uncertainty will be encountered, e.g., the selection of control points and the distance or the dissimilarity measures used for image matching. In this paper, we model these uncertainty in image registration using the theory of belief functions. By jointly using the pixel level and feature level information, more effective image registrations are accomplished. Experimental results, comparisons and related analyses illustrate the effectiveness of our evidential reasoning based image registration approach.**

***Keywords*—image registration; uncertainty; belief functions; evidential reasoning; dissimilarity.**

I. Introduction

The image fusion brings a more comprehensive and higher quality image information by jointly using the multi-sensor or multi-temporal images and that is why it has been widely used in civil [1] and military applications [2], [3]. The image registration [4], [5], [6] is a crucial step for the image fusion which can be performed either manually or automatically. In manual mode, human operators manually select the corresponding features in the images to be registered. To get a good image registration, the operator must select a large number of feature pairs across the whole images. Image registration techniques are mainly based on area-based and on feature-based analysis methods that can be used locally or globally [7]. Global approaches use the whole information of reference and sensed images to estimate the geometric transformations between the images. Local approaches, which are widely used in remote sensing image registration, compute the global mapping functions using few selected control points (CPs). Image registration requires several steps (matching, transform model estimation, re-sampling and final transformation) involving uncertainties on the choice of dissimilarity measures, of CPs, the level of fusion (pixel-level fusion versus feature-level fusion), etc. Various uncertainties enter in the image registration because of the choices of dissimilarity measures, the choice of CPs, the level we work at (pixel-level or feature-level), etc. In this work, we propose to use different dissimilarity measures as well as multi-source information such as pixel-level images and the features (e.g., the edge information) of the images to solve image registration. The method we propose is based on the belief functions (BF) [8] since BF are well adapted to model different types of uncertainties. After a detailed presentation of the new image registration technique proposed based on the evidential reasoning (ER), we present experimental results on real images. A comparative analysis with classical image registration methods is also done to show the improvement of performances of our proposed method.

II. Basics of Image Registration

The image registration [5] is required to compare or integrate the data obtained from different origins (different viewpoints, different times, different sensors, etc). The procedure of the image registration is summarized in Fig. 1 where each functional block is detailed in the sequel.

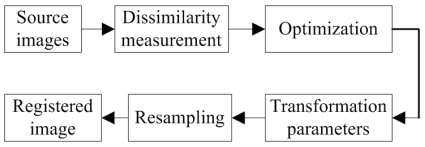

Fig. 1. Procedure of the image registration.

A. Source images

The (source) images of different origins include a reference image and the (sensed) images to be registered. The images can either be the original pixel-level information images, or transformed images (feature-level information). In non-automatic image registration, users always select some control points (CPs) extracted from the reference and sensed images for doing the image registration.

B. Dissimilarity measures

Several dissimilarity measures [9] can be used for the image registration. The main ones being the mutual information (MI) [10], the normalized correlation coefficient (NCC) [11], and the peak signal to noise ratio (PSNR) [12] defined as follows for images A and B with the same sizes $M \times N$:

1) Mutual Information (MI):

$$MI(A,B) = \sum_{a,b} p_{AB}(a,b) \log \frac{p_{AB}(a,b)}{p_A(a)p_B(b)} \tag{1}$$

where $p_A(a)$ is the probability of grey level a obtained from the grey histogram of image A, $p_B(b)$ is the probability of grey level b obtained from the grey histogram of image B and $p_{AB}(a,b)$ is the joint probability of grey level a in image A and b in image B.

2) Normalized Correlation Coefficient (NCC):

$$R(x,y) = \frac{\sum_{i,j}(A(x,y)-\bar{A})(B(x+i,y+j)-\bar{B})}{\sqrt{\sum_{i,j}(A(x,y)-\bar{A})^2 \sum_{i,j}(B(x+i,y+j)-\bar{B})^2}} \quad (2)$$

where $i = 1, ..., M; j = 1, ..., N$ and $\bar{A}, \bar{B}$ denote the average over the whole images of A and B, respectively.

3) Peak Signal to Noise Ratio (PSNR):

$$PSNR = 10 \times \log\left(\frac{255^2}{MSE}\right) \quad (3)$$

where 255 represents the maximum of the grey scale value in $[0, 255]$. MSE is the mean squared error defined as [13]

$$MSE = \frac{1}{M \times N}\sqrt{\sum_{i=1}^{M}\sum_{j=1}^{N}[A(i,j)-B(i,j)]^2} \quad (4)$$

C. Transformation

The transformation block refers to the elementary geometric spatial transformations between the reference image and the sensed image. It includes the rotation, the scaling and the translation transformations [4], [5], [6] and it is symbolically denoted T. The notation $(x, y) = T\{(s, t)\}$ means that an image defined over a (s, t) coordinate system is transformed to an image defined over a (x, y) coordinate system through the following geometrical elementary transformations:

1) The rotation of angle θ:

$$\begin{cases} x = s \cdot \cos\theta - t \cdot \sin\theta \\ y = s \cdot \sin\theta - t \cdot \cos\theta \end{cases} \quad (5)$$

2) The translation of parameters ds and dt:

$$\begin{cases} x = s + ds \\ y = t + dt \end{cases} \quad (6)$$

3) The scaling of parameters M_s and M_t:

$$\begin{cases} x = M_s \cdot s \\ y = M_t \cdot t \end{cases} \quad (7)$$

D. Optimization

The functional optimization block corresponds to the minimization of the mismatch errors in the image registration which are measured by the aforementioned dissimilarity measures. One wants to estimate the parameters M_s, M_t, ds, dt, and θ by minimizing a chosen objective function[1] $f(.,.)$

$$\min_{d_s,d_t,M_s,M_t,\theta} f(I_{ref}, T(I_{sensed})) \quad (8)$$

under the constraints

$$\begin{cases} 0 < d_s < M, 0 < d_t < N \\ M_s > 0, M_t > 0 \\ -\pi < \theta < \pi \end{cases} \quad (9)$$

where I_{ref} and I_{sensed} denote the reference image and the sensed image respectively. Because the objective function, i.e., the mismatch error is always non-convex, advanced optimization methods [14], or global optimization approaches are necessary (like genetic, or particle swarm algorithms, etc.)

[1]where $f(.)$ corresponds to a dissimilarity measure MI, NCC, or PSNR

E. Resampling

Resampling[2] is a crucial step for the grey-level image registration. The input image is resampled into the desired output map grid. The details of resampling are given in [4], [5], [6].

III. Uncertainties in Image Registration

As explained previously, the image registration is a crucial and difficult preliminary step for information fusion because the implementation of the optimization step always requires high computational cost. The possible low qualities and the large resolution difference of the images strongly impact registration performances, as well as the uncertainties about the choice of the control point and the dissimilarity measure.

A. Uncertainty in selection of control points

The performance of an image registration based on CPs always depends on the selection of CPs which is relatively subjective. Such an uncertainty may affect the results of the registration. Fig. 2 shows different CPs selected, and Table I show the estimation of parameters of T.

Fig. 2. Selection of different CPs.

TABLE I. Estimation of T Parameters using CPs of Fig. 2.

Transform parameters	between (a) and (b)	between (c) and (d)
Rotation (θ)	14.6465°	14.9024°
Scaling (M_s, M_t)	(0.9830, 0.9830)	(0.9935, 0.9935)
Translation(d_s, d_t)	(31.5075, -40.0214)	(31.0425, -40.3714)

B. Uncertainty in the choice of dissimilarity measures

The choice of the dissimilarity measure is also very important in image registration. Different dissimilarity measures always define or emphasize the dissimilarity from different aspects, so they could bring different matching degree between the reference image and the sensed images. Thus, the image registration results might also be influenced by the uncertainty caused by the selection of different dissimilarity measures.

To implement the image registration, several types of information such as the grey-level information and the feature-level information (e.g. the edge information) can be used.

[2]The resampling approach used in this paper is the bilinear interpolation

If we use the multiple types of information in an efficient manner, a better image registration performance is expected. In this paper, we propose to use belief functions to deal with different types of uncertainty and work at both grey-level and the feature-level of images in order to improve the performance of the image registration. Before presenting in details our new method, we recall some very basics on BF in the next section.

IV. Very Basics on Belief Functions

The belief functions have been introduced in [8] to reason under different types of uncertainties (epistemic and randomness). We consider a given discrete and finite frame of discernment (FOD) Θ with all mutually exclusive and exhaustive elements. A basic belief assignment (bba) $m(.)$ is defined as a mapping $m : 2^\Theta \rightarrow [0, 1]$ satisfying:

$$m(\emptyset) = 0 \quad \text{and} \quad \sum_{A \in 2^\Theta} m(A) = 1 \tag{10}$$

The belief $Bel(.)$ and the plausibility $Pl(.)$ functions are

$$\begin{cases} Bel(A) = \sum_{B \in 2^\Theta | \subseteq A} m(B) \\ Pl(A) = \sum_{B \in 2^\Theta | \cap B \neq \emptyset} m(B) \end{cases} \tag{11}$$

The combination of belief functions provided by several distinct sources can be done in many ways. Historically, Dempster's rule (denoted DS for short) has been proposed by Shafer in his DST [8]. DS rule has however been strongly criticized over the years for generating counter-intuitive results [15], for its dictatorial behavior [16], and for its incompatibiliy with Bayes fusion rule [17]. That is why other fusion rules have been developed to circumvent some of these drawbacks, in particular the more efficient (and complex) Proportional Conflict Redistribution Rule no. 6 (PCR6) [18] that will be also tested in this work. A detailed presentation of DS and PCR6 rules with many examples can be found in [18] and therefore they will not be presented here.

After combining the bba's by a given fusion rule we get a new bba denoted $m_{comb}(.)$. To make a decision on an element of the FOD Θ, we use a transformation to approximate m_{comb} in a probability mass function (pmf). Classically, the pignistic probability transformation $BetP(.)$ [19] proposed by Smets is used, but other transformations are also possible, like $DSmP(.)$ which is more complex to implement. Here, we use $BetP(.)$ only due to its simplicity. Details of $BetP(.)$, $DSmP(.)$ and other transformations are given in [18].

V. Evidential Reasoning for Image Registration

Two types of uncertainty can enter in the image registration:

- Uncertainty of Type 1: It comes from the choice of l different sets of control points that will yield estimations of T_1, T_2,...,T_l as shown in Fig. 3(a);
- Uncertainty of Type 2: It comes from the choice[3] of l different dissimilarities measures that will yield estimations of T_1, T_2,...,T_l as shown in Fig. 3(b).

[3]The number l of transformations involved in uncertainty of Type 2 is usually smaller than the number l of transformations involved in uncertainty of Type 1. We use the same notation here for convenience to denote the cardinality of the FOD, that is $|\Theta| = l$.

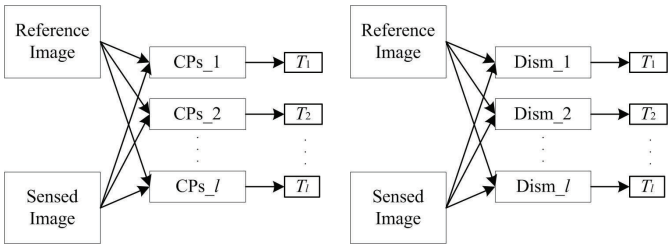

(a) Type 1(CPs). (b) Type 2 (Dissimilarities).

Fig. 3. Two types of uncertainty in image registration.

In this work, we don't deal with both types of uncertainty simultaneously[4]. We propose a method to work either with Type 1, or with Type 2 of uncertainty. Working with both types is currently under development and will be subject to future publications. The general principle of our evidential reasoning based image registration method is illustrated in Fig. 4. We

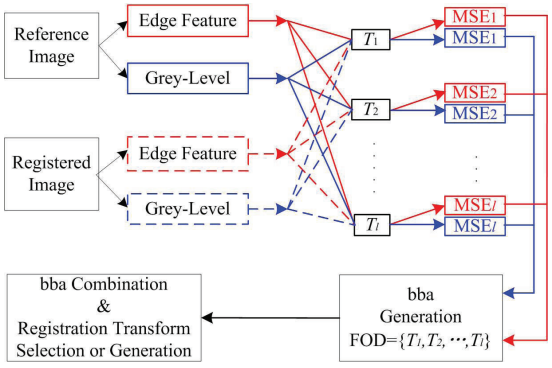

Fig. 4. Principle of image registration based on evidential reasoning.

work either with Type 1, or with Type 2 uncertainties (but not both) and we use both the grey-level information and the feature-level information (e.g., edge information) to obtain two MSE matching error scores. The set $\Theta = \{T_1, T_2, \ldots, T_l\}$ constitutes the FOD on which the two bba's to combine will be defined. One bba comes from the source processing the grey-level information (G), and the other bba comes from the source processing the feature-level information[5] (E). The generation of these bba's is detailed in the sequel. Then we combine these bba's by a fusion rule (DS or PCR6) to get the joint evaluation of all different transformations. From a probabilitic transformation, we estimate the pmf over the FOD from which we can either select the most likely transformation T_i of the FOD, or build a comprehensive transformation from all the transformations of FOD and their probability values.

A. Generation of bba's and their combination

The generation of bba's is based on the $MSE_i(G)$ and $MSE_i(E)$ score values of each transformation $T_i \in \Theta$, where G means Grey-level information, and E means Edge-level

[4]When we consider both type of uncertainty together, then we will have more transformations. For example, when there are m dissimilarity measures used and n sets of CPs used, we will have $m \cdot n$ transformations in total

[5]In this work, we use the edge feature.

information[6] (which is a particular feature level). These scores are normalized as follows

$$\begin{cases} MSE_i^R(G) = MSE_i(G)/\sum_{j=1}^{l} MSE_j(G) \\ MSE_i^R(E) = MSE_i(E)/\sum_{j=1}^{l} MSE_j(E) \end{cases} \quad (12)$$

From these normalized scores, we propose to build the bba's in two different manners: directly as Bayesian[7] bba's, or as non Bayesian bba's by the Fuzzy Cautious Ordered Weighted Average Evidential Reasoning (FCOWA-ER) approach [20].

• Generation of Bayesian bba's:

$$\begin{cases} m_G(\{T_i\}) = P_G(T_i) = \frac{e^{-1/MSE_i^R(G)}}{\sum_{j=1}^{l} e^{-1/MSE_j^R(G)}} \\ m_E(\{T_i\}) = P_E(T_i) = \frac{e^{-1/MSE_i^R(E)}}{\sum_{j=1}^{l} e^{-1/MSE_j^R(E)}} \end{cases} \quad (13)$$

The negative exponential function is used because the bigger the value of MSE, the worse the quality of the corresponding transformation. The combined mass function $m_c(.)$ is obtained by $m_c(.) = [m_G \oplus m_E](.)$, where $\oplus$ is the symbolic notation of the fusion operator (typically DS, or PCR6 fusion rules).

• Generation of Non-Bayesian bba's:

To generate Non-Bayesian bba's, we use the FCOWA-ER[8] method which consists in the following steps:
Step 1: Generation of the expected payoff matrix (EPM).

We calculate the expectation matrix defined by

$$E(T) = \begin{bmatrix} [e_{\min}(T_1), e_{\max}(T_1)] \\ \vdots \\ [e_{\min}(T_i), e_{\max}(T_i)] \\ \vdots \\ [e_{\min}(T_l), e_{\max}(T_l)] \end{bmatrix} \quad (14)$$

where $e_{\min}(T_i)$ and $e_{\max}(T_i)$ for $i = 1, 2, \ldots, l$ are given by

$$\begin{cases} e_{\min}(T_i) = \min\{e^{-1/MSE_i^R(G)}, e^{-1/MSE_i^R(E)}\} \\ e_{\max}(T_i) = \max\{e^{-1/MSE_i^R(G)}, e^{-1/MSE_i^R(E)}\} \end{cases} \quad (15)$$

Step 2: Normalization of the EPM.

The column-wise normalized expected payoff is given by

$$E^{norm}(T) = \begin{bmatrix} [e_{\min}^{norm}(T_1), e_{\max}^{norm}(T_1)] \\ \vdots \\ [e_{\min}^{norm}(T_i), e_{\max}^{norm}(T_i)] \\ \vdots \\ [e_{\min}^{norm}(T_l), e_{\max}^{norm}(T_l)] \end{bmatrix} \quad (16)$$

where

$$\begin{cases} e_{\min}^{norm}(T_i) = e_{\min}(T_i)/\max(e_{\min}(T_j)) \\ e_{\max}^{norm}(T_i) = e_{\max}(T_i)/\max(e_{\max}(T_j)) \end{cases} \quad (17)$$

In FCOWA-ER, the min and max bounds of $E^{norm}[T]$ are considered as two information sources, representing respectively the pessimistic and the optimistic attitudes. The two (min and max) columns of $E^{norm}(T)$ are interpreted as two fuzzy membership functions (FMFs) $\mu_{\min}(.)$ and $\mu_{\max}(.)$ representing the possibilities of all the alternatives: $T_1, ..., T_l$.

Step 3: From FMFs to bba's using α-cut.

We transform FMFs into bba's by using the classical α-cut approach [22]. More precisely, from any FMF $\mu(T_i)$, $i = 1, \ldots, l$ we sort $\mu(T_i)$ values by increasing order to get an order such that $0 < \alpha_1 < \alpha_2 < \cdots < \alpha_M \leq 1$ (the α-cuts).

$$m(B_j) = \frac{\alpha_j - \alpha_{j-1}}{\alpha_M} \quad (18)$$

where $B_j = \{T_i \in \Theta | \mu(T_i) \geq \alpha_j\}$. Applying this α-cut method to $\mu_{\min}(.)$, and to $\mu_{\max}(.)$ allows to get the corresponding bba's $m_1(.)$ and $m_2(.)$.

Step 4: Combination of $m_1(.)$ and $m_2(.)$.

$m_1(.)$ and $m_2(.)$ can be combined by any fusion rule (typically DS or PCR6) to get the joint evaluation of all different transformations, that is $m_c(.) = [m_1 \oplus m_2](.)$. Once $m_c(.)$ is computed, an evidential reasoning (ER) transformation method is used to estimate the best set of parameters $\{M_s, M_t, ds, dt, \theta\}$.

B. Generation of ER-based Transformation

Two methods (by maximum a posteriori (MAP), or by weighted average (WA)) can be used to estimate $\{M_s, M_t, ds, dt, \theta\}$ to provide the solution of the image registration problem based on evidential reasoning. These methods require the approximation[9] of the final combined bba $m_c(.)$ into a posterior probability measure $P_c(.)$ over Θ.

• Method 1: The solution $T^{\text{MAP}} = \{M_s, M_s, ds, dt, \theta\}$ corresponds to the parameters of the transformation T_i having the maximum a posteriori probability value. Index i is given by

$$i = \arg[\max_{j=1,\ldots,l} P_c(T_j)] \quad (19)$$

• Method 2 : The solution $T^{\text{WA}} = \{M_s, M_t, ds, dt, \theta\}$ corresponds to the weighted average of the parameters of all the transformations T_i with weighting factors $P_c(T_i)$. The parameters are given by

$$\begin{cases} \theta = \sum_{i=1}^{l} P_c(T_i) \cdot \theta^i \\ ds = \sum_{i=1}^{l} P_c(T_i) \cdot ds^i \\ dt = \sum_{i=1}^{l} P_c(T_i) \cdot dt^i \\ M_s = \sum_{i=1}^{l} P_c(T_i) \cdot {M_s}^i \\ M_t = \sum_{i=1}^{l} P_c(T_i) \cdot {M_t}^i \end{cases} \quad (20)$$

[6]The edge information of a given image is a binary image. Thus the MSE of edge feature (E) is in fact the MSE computed between the two corresponding binary images of the reference image and the sensed image to register.

[7]A bba is called Bayesian if all its focal elements are singletons of 2^Θ.

[8]FCOWA-ER is a modified version of COWA-ER [21]

[9]In this work we use $BetP(.)$ transformation.

VI. EXPERIMENTS

In this section we evaluate the new image registration method based on evidential reasoning using different configurations (using different sets of CPs or different dissimilarities, using DS and PCR6 fusion rules, using Bayesian and Non-Bayesian bba modelings, and using Method 1 or Method 2 for final decision making). The evaluation is done on different real images available on free image repositories [23].

A. Image registration using different CPs

In this analysis, the CPs are manually selected by using the function of *cpselect'* in Matlab. The sensed and the reference images have been magnified according to the same factor to be more accurate in the selection of CPs, that is why the coordinates of CPs have a decimal part. The origin of each image is at the up-left corner. x-axis is from left to the right and y-axis is from up to down.

• Results with the *Cameraman* images

Three different sets of CPs have been used as listed in TABLE II and shown in Fig. 5.

TABLE II. SETS OF CONTROL POINTS FOR *Cameraman* IMAGE

Sets of CPs	CPs on reference image	CPs on sensed image
Set 1	(168.8750, 73.8750)	(156.1250, 93.6250)
	(109.8750, 66.6250)	(103.3750, 83.6250)
	(32.8750, 108.8750)	(31.1250, 114.1250)
	(138.6250, 199.3750)	(118.8750, 204.1250)
Set 2	(105.1250, 38.8750)	(101.3750, 57.6250)
	(169.1250, 73.6250)	(155.8750, 93.8750)
	(22.8750, 190.3750)	(15.6250, 188.8750)
	(177.8750, 208.6250)	(152.6250, 215.6250)
Set 3	(124.1250, 78.625)	(115.1250, 95.3750)
	(162.1250, 63.6250)	(149.8750, 84.8750)
	(170.3750, 79.3750)	(156.6250, 99.8750)
	(116.6250, 209.1250)	(97.8750, 210.6250)
	(177.3750, 207.8750)	(153.1250, 215.8750)
	(132.1250, 199.6250)	(112.3750, 204.6250)

The sensed image is generated from the reference image using the following transformation parameters

$$T^{true} = \{\theta^{true} = 5.0^\circ, ds^{true} = 12.0, dt^{true} = 15.0, M_s^{true} = 0.90, M_t^{true} = 0.90\}$$

From the CPs in TABLE II, we obtain transformations T_1, T_2 and T_3 with corresponding parameters given in TABLE III.

TABLE III. TRANSFORMATIONS OBTAINED FOR *Cameraman* IMAGE.

Parameters	Translation: (ds, dt)	Rotation: θ	Scaling: (M_s, M_t)
T_1	(12.5506, 14.9714)	5.1601°	(0.9020, 0.9020)
T_2	(13.3836, 16.4005)	4.3291°	(0.8973, 0.8973)
T_3	(10.7417, 13.4381)	5.9321°	(0.9069, 0.9069)

Applying T_1, T_2, and T_3, we obtain the registration error (MSE) on grey-scale images and on the edge images listed in TABLE IV.

If we generate Bayesian bba's from these MSE values, then we get

$$m_G(T_1) = 0.3341, m_G(T_2) = 0.3346, m_G(T_3) = 0.3313;$$

(a) Original image CPs set 1 (b) Sensed image CPs set 1

(c) Original image CPs set 2 (d) Sensed image CPs set 2

(e) Original image CPs set 3 (f) Sensed image CPs set 3

Fig. 5. Sets of CPs on *Cameraman* image.

TABLE IV. MSE OF THE TRANSFORMATIONS

Transformations	Grey-Scale	Edge feature
T_1	0.01865	0.00125
T_2	0.01856	0.00121
T_3	0.01913	0.00126

$$m_E(T_1) = 0.3321, m_E(T_2) = 0.3364, m_E(T_3) = 0.3316;$$

Combining $m_G(.)$ and $m_E(.)$ with Dempster's rule, we get

$$m_c(T_1) = 0.3328, m_c(T_2) = 0.3377, m_c(T_3) = 0.3295;$$

Since $m_c(.)$ is a Bayesian bba, $BetP(T_i) = m_c(T_i)$. Therefore $T^{\text{MAP}} = T_2$ if Method 1 is used, or with Method 2

$$T^{\text{WA}} = \{\theta = 5.1310^\circ, ds = 12.2376, dt = 14.9505, M_s = 0.9021, M_t = 0.9021\}$$

If we use FCOWA-ER to generate Non-Bayesian bba's, one has

$$E(T) = \begin{bmatrix} [0.3321, 0.3341] \\ [0.3346, 0.3364] \\ [0.3313, 0.3316] \end{bmatrix}$$

The normalized expected possibility matrix will be

$$E^{norm}(T) = \begin{bmatrix} 0.3321/0.3346, 0.3341/0.3364 \\ 0.3346/0.3346, 0.3364/0.3364 \\ 0.3313/0.3346, 0.3316/0.3364 \end{bmatrix} = \begin{bmatrix} 0.9923, 0.9932 \\ 1.0000, 1.0000 \\ 0.9899, 0.9857 \end{bmatrix}$$

Using α-cut, we get the two bba's as follows

TABLE V. $m_1(.)$ AND $m_2(.)$ BBA'S.

Focal elem. & bba's	$m_1(.)$	$m_2(.)$
T_2	0.0077	0.0068
$T_1 \cup T_2$	0.0020	0.0075
$T_1 \cup T_2 \cup T_3$	0.9899	0.9857

Combining $m_1(.)$ and $m_2(.)$ by Dempster's rule gives

$m_c(T_2) = 0.0114, m_c(T_1 \cup T_2) = 0.0098, m_c(T_1 \cup T_2 \cup T_3) = 0.9757.$

Using $BetP(.)$ transformation, we get

$BetP(T_1) = 0.3302, BetP(T_2) = 0.3446, BetP(T_3) = 0.3252.$

Therefore, $T^{\text{MAP}} = T_2$ with method 1, and with Method 2

$$T^{\text{WA}} = \{\theta = 5.1220^\circ, ds = 12.2511, dt = 14.9669, \\ M_s = 0.9020, M_t = 0.9020\}.$$

A similar analysis has been done using PCR6 fusion rule instead Dempster's rule. The performances of the different methods evaluated with the MSE criteria using T^{WA} solutions are shown on Fig. 6. As we can see in Fig. 6, image registration approach based on evidential reasoning performs better than the single transformations obtained by using different CPs. Approximately, the MSE can be reduced by 10%–15%. In the legend of Fig. 6, B-bba(DS) and FCOWA(DS) means respectively Bayesian bba modeling and Non-Bayesian bba modeling, combined with Dempster's rule. B-bba(PCR6) and FCOWA(PCR6) have the same meaning when replacing Dempster's rule by PCR6 rule.

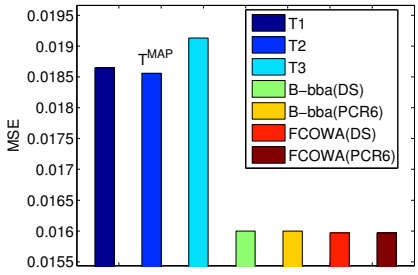

Fig. 6. MSE performances of *Cameraman* images registration.

• Results with the *Tai-Lake* images

We did a similar analysis on *Tai-Lake* images [10] with three sets of CPS shown in Fig. 7. The transformations T^{WA} obtained by using the different sets of CPs with PCR6 and Dempster's rule, and with Bayesian and Non-Bayesian bba modelings are listed in Table VI. The last row of TABLE VI (and of the next Tables) corresponds to the true parameters that have been used to generate the sensed image from the reference image. By using different transformations obtained respectively on the sensed image in grey scale, we can calculate the error with the reference image. The MSE performances of the image registration solutions are illustrated in Fig. 8. As we can see in Fig. 8, the image registration based on evidential reasoning performs better than the single transformations obtained by using different each set of CPs. Approximately, MSE value can be reduced by 3%-8% with our image registration approach. $T^{\text{MAP}} = T_1$ is also noted in Fig. 8.

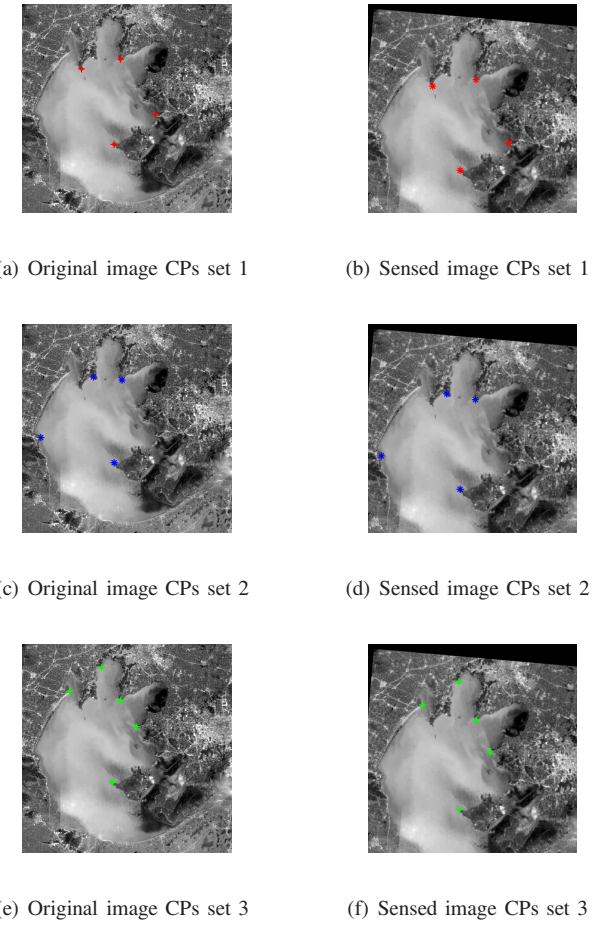

(a) Original image CPs set 1 (b) Sensed image CPs set 1

(c) Original image CPs set 2 (d) Sensed image CPs set 2

(e) Original image CPs set 3 (f) Sensed image CPs set 3

Fig. 7. Images of 'Tai-lake'

TABLE VI. TRANSFORMATIONS OBTAINED FOR IMAGES OF 'TAI-LAKE'.

Parameters	Translation: (ds, dt)	Rotation: θ	Scaling: (M_s, M_t)	MSE
T_1	(11.5307, 7.7504)	5.9084°	(1.1000, 1.1000)	0.01900
T_2	(8.0331, 9.5284)	4.1219°	(1.1031, 1.1031)	0.01988
T_3	(13.7849, 6.3897)	5.5632°	(1.7037, 1.7037)	0.01973
B-bba (DS)	(11.1262, 7.2188)	5.2073°	(1.0922, 1.0922)	0.01815
B-bba (PCR6)	(11.1262, 7.2198)	5.2059°	(1.0922, 1.0922)	0.01815
FCOWA (DS)	(11.1336, 7.2202)	5.2145°	(1.0923, 1.0923)	0.01815
FCOWA (PCR6)	(11.1336, 7.2202)	5.2145°	(1.0923, 1.0923)	0.01815
true	(10.0000, 7.0000)	5.0000°	(1.1000, 1.1000)	

[10]It can be downloaded from http://baike.baidu.com/view/1596.htm

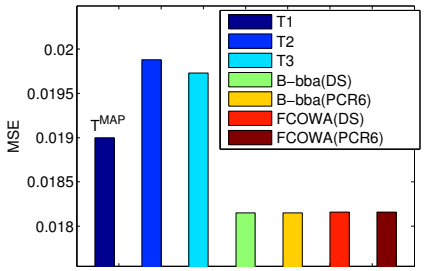

Fig. 8. MSE performances for the registration of Tai-lake images.

B. Image registration using different dissimilarity measures

Here, only the uncertainty of Type 2 related to the choice of different dissimilarity measures is considered. The grey level information of the images is used in the registration and we don't use CPs. Only the Method 2 (Weighted Average) based on Eq. (20) is used in our analysis to give the solution of the image registration.

• Results with the *Brain* images

The reference and sensed *Brain* images are shown in Fig. 9. In this experiment, there is no scaling. The dissimilarities

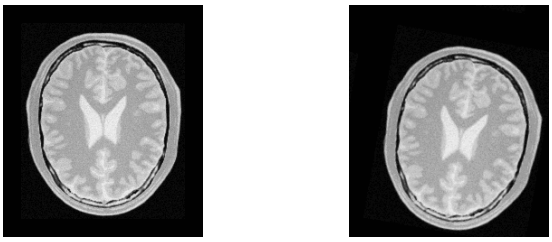

(a) Reference image. (b) Sensed image.

Fig. 9. Brain images used for the registration.

TABLE VII. TRANSFORMATIONS OBTAINED FOR IMAGES OF 'BRAIN'.

Parameters	Translation: (ds, dt)	Rotation: θ	MSE
T_1 (MI)	(13.0667, 16.0296)	9.8862°	0.01472
T_2 (NCC)	(13.0484, 15.9586)	9.9108°	0.01457
T_3 (PSNR)	(12.9924, 15.9951)	10.1666°	0.01474
B-bba (DS)	(13.0360, 15.9786)	9.9871°	0.01431
B-bba (PCR6)	(13.3060, 15.9786)	9.9872°	0.01431
FCOWA-ER(DS)	(13.0361, 15.9786)	9.9865°	0.01431
FCOWA-ER(PCR6)	(13.0361, 15.9786)	9.9865°	0.01431
true	(13.0000, 16.0000)	10.0000°	

measures MI, NCC, PSNR are used as optimization criteria for image registration using grey-scale level. Therefore three different types of transformations T_1, T_2, and T_3 are obtained. According to the grey-scale level, and edge information our image registration method is applied using either Bayesian or Non-Bayesian bba's modelings, and either Dempster's or PCR6 rules. The estimations of parameters of the T^{WA} solutions are given in TABLE VII following the steps listed in Section V. The MSE performances of different solutions are illustrated in Fig. 10. As we can see in Fig. 10, our image registration approach based on evidential reasoning performs better than the single transformations obtained by using different dissimilarity measures. Approximately, the MSE values can be reduced by 0.7%-1.7% with this new registration technique. $T^{\text{MAP}} = T_2$ is also noted in Fig. 10.

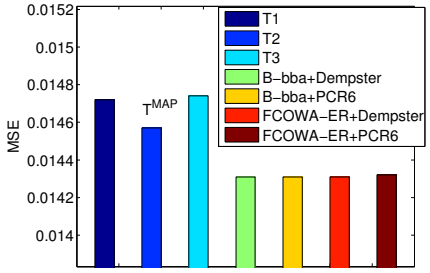

Fig. 10. MSE performances for registration of Brain images.

• Results with the *City* images

(a) Referencel image (b) Sensed image

Fig. 11. City Images used for the registration.

We consider the City images shown in Fig. 11. In this experiment, there is no scaling. Here MI, NCC, PSNR are used respectively in image registration (grey-scale level). According to the grey-scale, and edge information our image registration method is applied using either Bayesian or Non-Bayesian bba's modelings, and either Dempster's or PCR6 rules. The estimations of parameters of the T^{WA} solutions are given in TABLE VIII following the steps explained in Section V. The

TABLE VIII. TRANSFORMATIONS OBTAINED FOR IMAGES OF 'CITY'.

Parameters	$Translation: (ds, dt)$	$Rotation: \theta$	MSE
T_1 (MI)	(6.7855, 9.4382)	8.9282°	0.01293
T_2 (NCC)	(6.5750, 8.7618)	8.9282°	0.01206
T_3 (PSNR)	(6.2504, 8.5016)	8.9220°	0.01434
B-bba (DS)	(6.5420, 8.9061)	8.9366°	0.01116
B-bba (PCR6)	(6.5408, 8.9047)	8.9344°	0.01117
FCOWA (DS)	(6.5451, 8.9084)	8.9348°	0.01115
FCOWA (PCR6)	(6.5451, 8.9084)	8.9348°	0.01115
true	(6.0000, 9.0000)	9.0000°	

MSE performances of different T^{WA} solutions are illustrated in Fig. 12. We see that our image registration approach based on evidential reasoning performs better than the single transformations obtained by using different dissimilarity measures. Approximately, the MSE values can be reduced by 8%-12%. $T^{\text{MAP}} = T_2$ is also noted in Fig. 12.

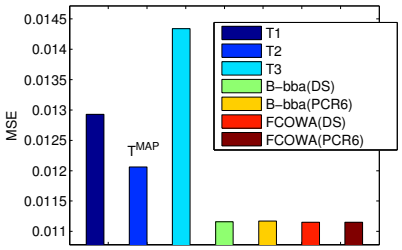

Fig. 12. MSE performances for registration of City images.

From all the experiments done, we see that bba's modelings do not affect strongly the MSE performances. Our analysis shows that FCOWA Non-Bayesian bba modeling is the best choice. One sees also that the choice of the combination rule does not affect seriously the MSE performances because the effect of the fusion rule is lower compared with the diversity of the different information sources. In our approach, the diversity originates from the different levels of information used (i.e. the grey-scale level and the feature level).

VII. Conclusions

In this paper, a new image registration method based on evidential reasoning is developed. Two types of uncertainty that can enter in the image registration are taken into account and modeled by belief functions. The information of grey-level and edge feature are jointly used to provide a better solution to the image registration problem thanks to basic belief assignments (bba's) modelings and fusion rules. The experimental results show that this new approach improves the precision of the image registration. The generation of bba's is crucial in the applications involving belief functions but there is no general theoretical method for bba generation. In this paper, we have proposed, in the image registration context, two bba's modelings (Bayesian, and Non-Bayesian) and we have evaluated their performances. It should be noted that although what we have used are all grey-scale images, our proposed approach can also be easily applied to the color images. At least we can homogenize and normalize the different color maps, i.e., convert color images to grey-scale images. Then the technique proposed as for grey images can also work. In future, we will work on the direct use of color images in evidential reasoning based image registration. In this work, the proposed image registration method works independently with each type of uncertainty (the uncertainty in the choice of sets of CPs, or the uncertainty in the choice of dissimilarity measures). A global image registration method dealing simultaneously with both types of uncertainty is under development and will be presented in a forthcoming publication.

Acknowledgment

This study was co-supported by Grant for State Key Program for Basic Research of China (973) (No. 2013CB329405), National Natural Science Foundation of China (No.61104214, No. 61203222), Foundation for Innovative Research Groups of the National Natural Science Foundation of China (No. 61221063), China Postdoctoral Science Foundation (No. 20100481337, No.201104670), Specialized Research Fund for the Doctoral Program of Higher Education (No. 20120201120036), and Fundamental Research Funds for the Central Universities (No.xjj2012104).

References

[1] M. S. Holia, "Mutual information based image registration for MRI and CT SCAN brain images", In Proc. of ICALIP 2012, July 16-18, 2012, Shanghai, China, p. 78–83.

[2] R. A. Schowengerdt, *Remoting Sensing: Models and Methods for Image Processing (3rd Ed.)*, Academic Press, Waltham, MA, USA, 2006.

[3] A. Wong, D. A. Clausi, "ARRSI: Automatic registration of remote-sensing images", IEEE Trans. on GRS, vol. 45, no. 5, p. 1483–1493, 2007.

[4] L. G. Brown, "Survey of Image Registration Techniques", ACM Computing Surveys, vol. 24, no. 4, p. 325–376, 1992.

[5] B. Zitova, J. Flusser, "Image registration methods: a survey, Image and Vision Computing", vol. 21, no. 11, p. 977–1000, 2003.

[6] M. Deshmukh, U. Bhosle, "A survey of image registration", Int. J. of Image Processing, vol. 5, no. 3, p. 245–269, 2011.

[7] S. R. Panchal, S. K. Shah, "A survey: methods of feature based image registration", Int. J. of ECCE, vol. 3, no. 4, p. 787–797, 2012.

[8] G. Shafer, *A Mathematical Theory of Evidence*, Princeton University Press, 1976.

[9] G. J. Wen, J. J. Lv, W. X Yu, "A high-performance feature-matching method for image registration by combining spatial and similarity information", IEEE Trans. on GRS, vol. 46, no. 4, p. 1266–1277, 2008.

[10] H. M. Chen, P. K. Varshney, M. K. Arora, "Performance of mutual information similarity measure for registration of multitemporal remote sensing images", IEEE Trans. on GRS, vol. 41, no. 11, p. 2445–2454, 2003.

[11] L.D. Stefano, S. Mattoccia, M. Mola, "An efficient algorithm for exhaustive template matching based on normalized cross correlation", In Proc. of ICIAP'03, Sept 11-13, 2003, Naples, Italy, p. 322–327.

[12] Q. Huynh-Thu, M. Ghanbari, "Scope of validity of PSNR in imageideo quality assessment", Electronics Letters, vol. 44, no. 13, p. 800–801, 2008.

[13] A. M. Eskicioglu, P. S. Fisher, "Image quality measures and their performance", IEEE Trans. on Comm., vol. 43, no. 12, p. 2959–2965, 1995.

[14] D. T. Pham, *Intelligent Optimisation Techniques*, Springer, 2000.

[15] L. A. Zadeh, "A simple view of the Dempster-Shafer theory of evidence and its implication for the rule of combination", AI magazine, vol. 2, no. 7, p. 85–90, 1986.

[16] A. Tchamova, J. Dezert, On the behavior of Dempster's rule of combination and the foundations of Dempster-Shafer theory, (Best paper award), in Proc. of the 6th IEEE Int. Conf. on Intelligent Systems, Sept. 2012, Sofia, Bulgaria.

[17] J. Dezert,A. Tchamova, D. Han, J.-M. Tacnet, "Why Dempster's fusion rule is not a generalization of Bayes fusion rule", submitted to Fusion 2013 Int. Conf., Istanbul, July 2013.

[18] F. Smarandache, J. Dezert (Editors), *Applications and Advances of DSmT for Information Fusion (Vol III)*, American Research Press, Rehoboth, NM, USA, 2009. URL: fs.gallup.unm.edu/DSmT.htm

[19] P. Smets, "The transferable belief model", Artifical Intelligence, vol. 66, no. 2, p. 191–234, 1994.

[20] D. Q. Han, J. Dezert, J.-M. Tacnet, C. Han, "A fuzzy-cautious OWA approach with evidential reasoning", in Proc. of Fusion 2012 Int. Conf., July 9-12, 2012, Singapore, p. 278–285.

[21] J.-M. Tacnet, J. Dezert, "Cautious OWA and evidential reasoning for decision making under uncertainty", in Proc. of Fusion 2011 Int. Conf., July 5-8, 2011, Chicago, IL, USA, p. 2074–2081.

[22] M. C. Florea, A.-L. Jousselme, D. Grenier, É. Bossé, "Approximation techniques for the transformation of fuzzy sets into random sets", Fuzzy Sets and Syst., vol. 159, no. 3, p. 270–288, 2008.

[23] Open Image data bases. URL: http://links.uwaterloo.ca/Repository.html http://www.imageprocessingplace.com